Unmanned Systems, Vol. 10, No. 2 (2022) 147–157

DOI: 10.1142/S230138502250008X

UNMANNED SYSTEMS
https://www.worldscientific.com/worldscinet/us

A Virtual Method to Estimate the Aerodynamic Coefficients of UAV

Zaouche Mohammed[*,†], Foughali Khaled[*]

[*]*Ecole Militaire Polytechnique, Bordj El Bahri,*
Alger 16000, Algeria

In this work, a new approach for aircraft aerodynamic behavior identification by using virtual simulation is proposed. Both theoretical and experimental aspects are presented. A simulation environment, Microsoft Flight Simulator, is used as the test platform. To make the communication with this environment possible, a real-time interface that allows the read and/or write from and to the shared memory layer of this flight simulator is developed. Using this interface, the virtual aircrafts sensors are read and the commands are written to the inputs control (thrust, elevators, ailerons, trims, and rudder). Also, an identification of the aerodynamic coefficients' derivatives using the total least square technique is presented. The piloting law expression is toughly tied to those derivatives which are unknown and not always available. The aircraft aerodynamic model is then used to calculate the aerodynamic coefficients. We determine the aerodynamic performances of the wing which is based on the polar drag, the computation of the maximum lift-to-drag coefficient ratio and the determination of the moment in which the aerodynamic stall phenomenon appears.

Keywords: Aerodynamic performance; adaptive differentiator sliding mode; virtual simulation platform; MicroSoft flight simulator universal inter-process communication FSUIPC; predator UAV; polar drag; total least squares estimation technique.

1. Introduction

The use of aerodynamic coefficients for the characterization of the behavior of an aircraft in flight remains one of the oldest and most emergent research projects. Identifying these coefficients is a complex and challenging task in the frame of aerodynamic modeling. To be able to estimate all the aerodynamic parameters, the complexity of their descriptions must be coherent with the application but also with the available data [1–4].

The determination of the aerodynamic parameters from free flight data can be formulated as a system identification problem. In this paper, an identification procedure of the aerodynamic coefficients' derivatives using the Total Least Square Technique (TLSE) is presented. A new approach for aircraft aerodynamic behavior identification using virtual simulation environment is proposed.

Also, the aerodynamic performances of the wing are determined using the polar drag, the computation of the maximum lift-to-drag coefficient ratio and the determination of the appearance moment of the aerodynamic stall phenomenon. The drag polar is the rapport between the lift and its resulting drag. It can be represented by an equation of the ratio of the lift coefficient to the drag coefficient, or just displayed as the so-called a polar plot diagram.

2. Problem Statement

The main objective of this paper is to identify the aerodynamic model of an aircraft flying in a virtual environment.

We use MicroSoft Flight Simulator (MSFS) as simulated world environment coupled to a hardware and software development platform. MSFS is developed by Microsoft, with several simulated aircrafts included in its airplane library. We chose the Predator MQ1, a reconnaissance and attack UAV (Fig. 1).

The main goal is to identify the aircraft aerodynamic performances; and to do so, we propose the following approach:

- Implementation of a real-time interface between the MSFS and the module RTWT (Real Time Windows Target) of Simulink/Matlab;

Received 20 September 2020; Accepted 9 July 2021; Published 28 August 2021. This paper was recommended for publication in its revised form by editorial board member, Biao Wang.
Email Address: †*zaouchemohamed@yahoo.fr*

Fig. 1. UAV and environment visualization.

- Presentation of the system aerodynamic model;
- Development and implementation of the aircraft aerodynamic model;
- Determination of the aerodynamic performance of the wing which is based on the polar drag, polar lift and the determination of the moment in which the aerodynamic stall phenomenon appears;
- Identification of the aerodynamic coefficients' derivatives, by means of the Total Least Square Estimation (TLSE) technique;
- Flight tests.

3. MicroSoft Flight Simulator

MSFS is a software developed by Microsoft. Its latest versions, Flight Simulators FS2004 and FSX, are considered as a virtual environment dedicated to pilots.

The open architecture presented by MSFS is a very important aspect that makes possible its expansion by the integration of new aircraft models (add-ons). It also enables the development of external software and hardware modules communicating with the environment via Application Programming Interfaces (APIs), interaction models or communication protocols.

These software extensions are based on the use of Flight Simulator Universal Inter-Process Communication (FSUIPC) APIs for MSFS-2004 and SimConnect for FSX. The communication is interpreted by the possibility of the real-time reading and writing in the MSFS virtual environment (see Figs. 2) [5–7].

4. Characteristics of the MQ-1 Predator

We have a way in flight dynamic characteristics by means of the *Airwrench* tool (mudpond.org/AirWrench/main.htm). This software gives possibility of creating and adjusting flight dynamics of the simulated plane models. This tool uses aerodynamics formulas and dynamic flight equations. It calculates aerodynamic coefficients based on the real characteristics of the aircraft (Table 1).

Table 1. MQ-1 predator simulated characteristics given by means of the Airwrench tool.

Dimensions	Moments of inertia
Length: 11.88 m	Pitch: Iyy = 1800.00
Wingspan (b): 14.84 m	Roll: Ixx = 3700.00
Wing surface area (S): 11.43 m^2	Yaw: Izz = 1800.00
Wing root chord (c): 1.55 m	Cross: Ixz = 0.00
Aspect ratio: 19.27	
Taper ratio: 0.10	
Oswald efficiency factor: 0.680	
Elevator area: 1.54 m^2	
Rudder area: 0.62 m^2	
Aileron area: 1.70	

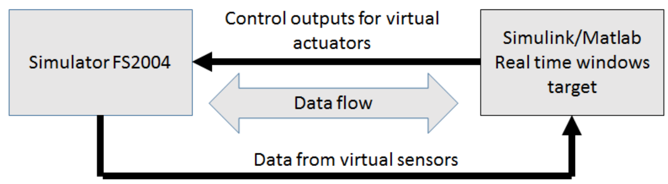

Fig. 2. Block diagram of the software environment design.

AirWrench is a software tool for creating flight dynamics for MSFS. It compiles a complete 'air' file used by the MSFS based on the physical dimensions and performance specifications of the real aircraft.

The flight dynamics of MSFS are defined in two files: a binary file having the extension '.air', and a text file named 'aircraft.cfg'. AirWrench considers these two files as a single flight dynamics file set.

5. Implementation of a Real-Time Interface Between MSFS and the Module RTWT of Simulink/Matlab

We design our Software to interface the simulated aircraft in Flight Simulator environment (read and/or write many sensors, actuators data and parameters).

The FSUIPC dynamic library is used for the communication with FS2004. This library created by Peter Dowson is downloadable from his website (www.schiratti.com/dowson.html). It permits external process to read and write in and from MSFS by means of an InterProcess Communication (IPC) using a buffer of 64 Kbyte.

The applications that use FSUIPC are based on the following algorithm (see Fig. 3) witch we exploited to implement our programs in C++.

The documentation given with FSUIPC explains the organization of this buffer. To read or write a variable using

February 11, 2022 2:26:19pm WSPC/284-US 2250008 ISSN: 2301-3850 2nd Reading

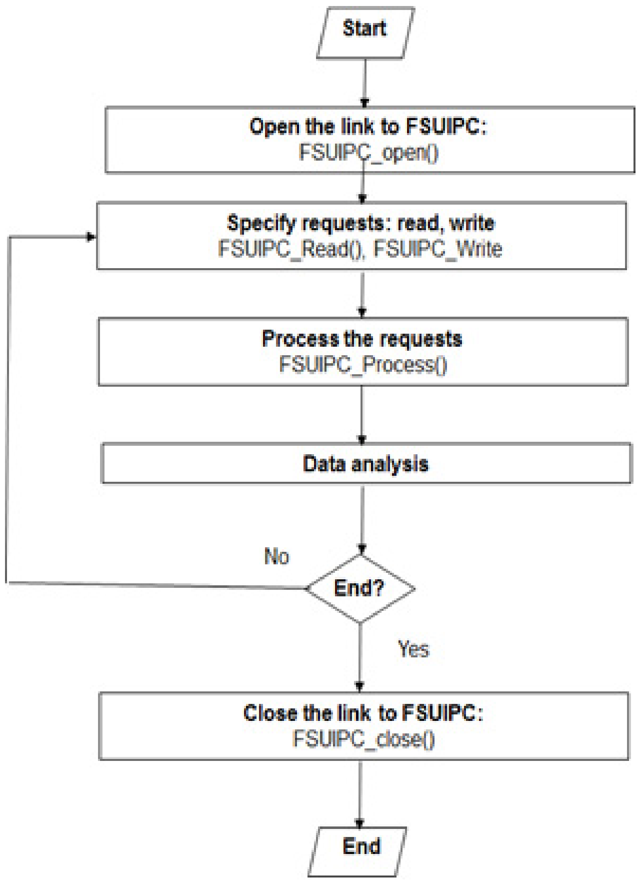

Fig. 3. Communication algorithm using FSUIPC.

the FSUIPC, we need to know its offset address, its format, and the necessary conversions. For example, the speed IAS (V) is read as a signed long S32 at the offset 002BC. Figure 4 shows the parameters used in our simulation.

To do this, we emulate the sensors through the following steps:

- Set the timer's sampling frequency T_i;
- Determine the FSUIPC address where sensor data begins OFFSETmin[i];

Address	Name	Var.Type	Size (octet)	Usage
30B0	Roll rate (p)	double	8	$\frac{rad}{s}$
30A8	Pitch rate (q)	double	8	$\frac{rad}{s}$
30B8	Yaw rate (r)	double	8	$\frac{rad}{s}$
3060	Acceleration (a_x)	double	8	ft/s^2
3068	Acceleration (a_y)	double	8	ft/s^2
3070	Acceleration (a_z)	double	8	ft/s^2
02BC	Indicated Air Speed (V)	Int	4	$Knot * 128$
2ED0	Incidence (α)	double	8	$Radian$
2ED8	Incidence (β)	double	8	$Radian$
0BB2	Elevator deflection (δ_e)	short	2	-16383 to +16383
0BB6	Aileron deflection (δ_a)	short	2	-16383 to +16383
0BBA	Rudder deflection (δ_r)	short	2	-16383 to +16383
088C	Thrust control (δ_x)	short	2	-16383 to +16383

Fig. 4. Flight parameters in the buffer FSUIPC.

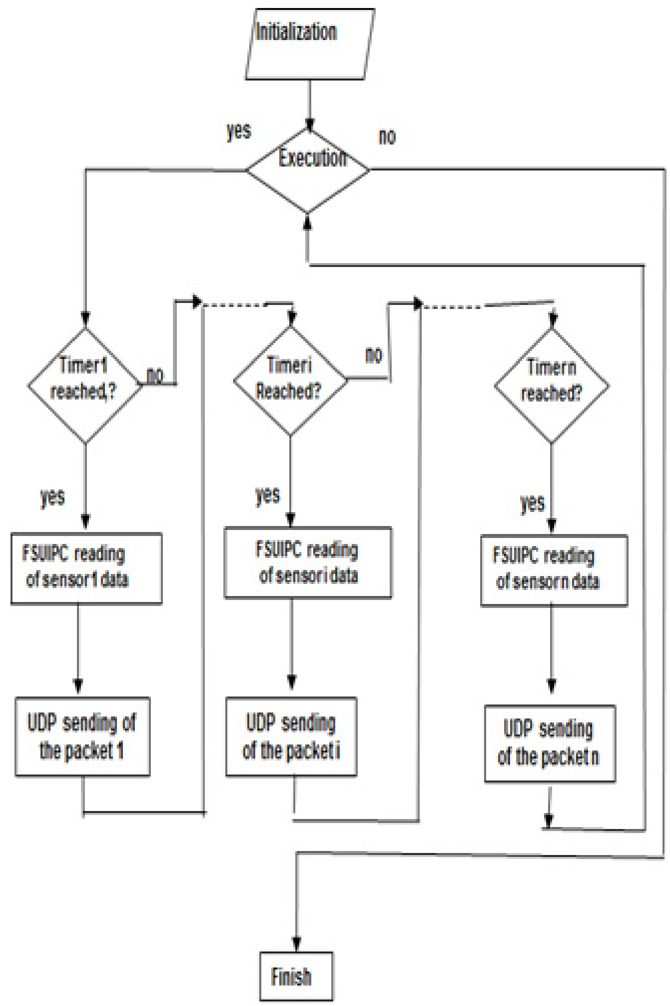

Fig. 5. Algorithm FSUIPC reading sensors data.

- Set the size of its data: SizeData[i];
- As shown in Fig. 5, the developed code in C + + performs a scan to check if a "Timer" has reached its period. Then, it reads the FSUIPC data related to the sensor (knowing the memory offset), forms its packet and sends it using UDP.

6. Software in the Loop Methodology

We propose an environment framework based on a software in the loop (SIL) methodology (Fig. 6) and we use MSFS–2004 as a plane simulation environment.

This work is a real-time virtual simulation, we read or/and write the desired parameters from and to MSFS through the computer memory by using the FSUIPC library.

We start by running the MSFS and the interface that communicates with the module RTWT of Simulink/Matlab.

In a first step, we used the predator. The take-off was done using the keyboard. Then, we run our software to

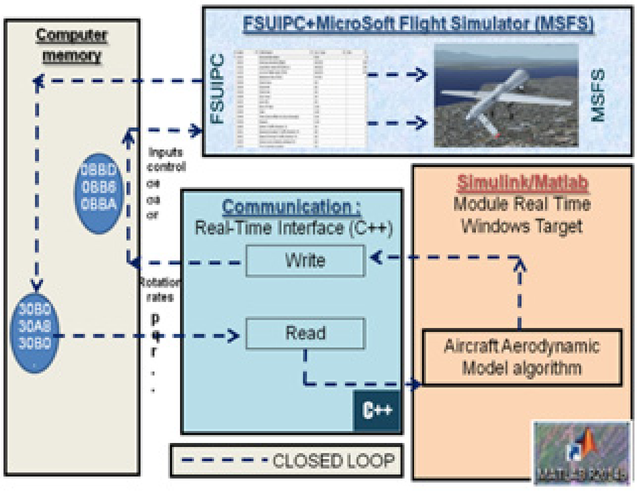

Fig. 6. SIL architecture.

transmit the control inputs to the autopilot controller in order to maintain the desired trajectory.

7. Identification Procedure of Aerodynamic Coefficients

The aerodynamic forces and moments depend on the following factors: angle of attack α, angle of sideslip β, deflection of directional control surface, deflection of lateral control surface, Much number and Reynolds number [8–10].

7.1. *Longitudinal aerodynamic forces and moments*

All expressions for the longitudinal steady-states aerodynamic forces and moments in matrix format are presented by

$$\begin{bmatrix} F_{ax} \\ F_{az} \\ M \end{bmatrix} = \begin{bmatrix} -D \\ -L \\ M \end{bmatrix} = \begin{bmatrix} -C_D.Q.S \\ -C_L.Q.S \\ C_m.Q.S.c \end{bmatrix}, \tag{1}$$

V is the true airspeed m/s, ρ is the air density Kg/m^3, $Q = 0,5.\rho.V^2$ is the dynamic pressure.

S is the wing surface area, D is the total airplane drag force, L is the total airplane lift force, M is the airplane pitching moment and c is the mean aerodynamic chord (m^2).

The aerodynamic forces and moments coefficients C_D, C_L, C_m in matrix format are presented by

$$\begin{bmatrix} C_D \\ C_L \\ C_m \end{bmatrix} = \begin{bmatrix} C_{D_0} & C_{D_\alpha} & C_{Di_H} & C_{Dq} & C_{D\delta_e} \\ C_{L_0} & C_{L_\alpha} & C_{Li_H} & C_{Lq} & C_{L\delta_e} \\ C_{m_0} & C_{m_\alpha} & C_{mi_H} & C_{mq} & C_{m\delta_e} \end{bmatrix} \begin{bmatrix} 1 \\ \alpha \\ i_H \\ \dfrac{qc}{V} \\ \delta_e \end{bmatrix}. \tag{2}$$

C_{D0}, C_{L0} and C_{m0} are the total airplane drag, lift and pitching moment coefficients, respectively, for $\alpha = i_H = \delta_e = 0$.

$C_{D\alpha}$, $C_{L\alpha}$ and $C_{m\alpha}$ are the total airplane drag, lift and pitching moment coefficients change with angle of attack at $i_H = \delta_e = 0$.

C_{Di_H}, C_{Li_H} and $C_{D\delta_e}$ or $C_{L\delta_e}$, $C_{m\delta_e}$ and C_{mi_H} are the total airplane drag, lift and pitching moment coefficients change with stabilizer or elevator angle δ_e at $\alpha = 0$.

7.2. *Lateral aerodynamic forces and moments*

All expressions for the lateral steady-states aerodynamic forces and moments in matrix format are presented by

$$\begin{bmatrix} l \\ F_{ay} \\ N \end{bmatrix} = \begin{bmatrix} C_l.Q.S.b \\ C_y.Q.S \\ C_n.Q.S.b \end{bmatrix}, \tag{3}$$

where l is the total airplane rolling moment, F_{ay} is the total airplane aerodynamic side force, N is the airplane yawing moment and b is the wing span.

$$\begin{bmatrix} C_l \\ C_y \\ C_n \end{bmatrix} = \begin{bmatrix} C_{l_\beta} & C_{lp} & C_{lr} & C_{l\delta_a} & C_{l\delta_r} \\ C_{y_\beta} & C_{yp} & C_{yr} & C_{y\delta_a} & C_{y\delta_r} \\ C_{n_\beta} & C_{np} & C_{nr} & C_{n\delta_a} & C_{n\delta_r} \end{bmatrix} \begin{bmatrix} \beta \\ \dfrac{pb}{2V} \\ \dfrac{rb}{2V} \\ \delta_a \\ \delta_r \end{bmatrix}. \tag{4}$$

The above equations can be transformed in the wind axe:

$$\begin{aligned} C_D &= -C_x.\cos(\alpha)\cos(\beta) \\ &\quad - C_y.\sin(\beta) - C_z.\sin(\alpha).\cos(\beta), \\ C_L &= -C_x.\sin(\alpha) - C_z.\cos(\alpha), \\ C_{yw} &= -C_x.\cos(\alpha)\sin(\beta) + C_y.\cos(\beta) \\ &\quad - C_z.\sin(\alpha).\sin(\beta). \end{aligned} \tag{5}$$

7.3. *Structuring the aerodynamic data base*

The aircraft sensor measurements are matched to the aerodynamic coefficients through a mathematical model.

$$\begin{aligned} C_x &= \frac{\begin{aligned} &m[a_x.\cos(\alpha)\cos(\beta) + ay.\sin(\beta) \\ &\quad + a_z.\sin(\alpha).\cos(\beta)] - F_p.\cos(\alpha)\cos(\beta) \end{aligned}}{Q.S}, \\ C_z &= \frac{m[-a_x.\sin(\alpha) + a_z.\cos(\alpha)] + F_p.\sin(\alpha)}{Q.S}, \\ C_y &= \frac{\begin{aligned} &m[-a_x.\cos(\alpha)\sin(\beta) \\ &\quad + a_y.\cos(\beta) - a_z.\sin(\alpha).\sin(\beta)] \\ &+F_p.\cos(\alpha).\sin(\beta) \end{aligned}}{Q.S}, \end{aligned} \tag{6}$$

$$\begin{aligned} C_l &= \frac{\dot{p}.I_{xx} + q.p.(I_{zz} - I_{yy}) - (p.q + \dot{r}).I_{zz}}{Q.S.b}, \\ C_m &= \frac{\dot{q}.I_{yy} + r.p.(I_{xx} - I_{zz}) + (p^2 - r^2).I_{xz} - \triangle F_p}{Q.S.c}, \\ C_n &= \frac{\dot{r}.I_{zz} + q.p.(I_{yy} - I_{xx}) + (r.q - \dot{p}).I_{zz}}{Q.S.b}, \end{aligned} \quad (7)$$

where F_p is the propulsion force expressed in the body frame [9]:

$$F = F_p \begin{bmatrix} \cos(\beta)\cos(\alpha) \\ \sin(\beta) \\ \cos(\beta)\sin(\alpha) \end{bmatrix} \sigma_t = \frac{K_m \eta}{V_a}, \quad (8)$$

where V_a is the aerodynamic speed, η is the turbo jet constant and σ_t is the throttle position with a value between 0 and 1.

7.3.1. *Estimated angular accelerations $\dot{p}$, $\dot{q}$ and $\dot{r}$ using adaptive differentiator sliding mode technique*

The calculation of the aerodynamic coefficients C_l, C_m and C_n from Eq. (7) requires knowledge of the angular accelerations values $\dot{\omega} = \begin{bmatrix} \dot{p} & \dot{q} & \dot{r} \end{bmatrix}^T$. Therefore, none of the aircraft sensors can provide angular accelerations signal $\dot{p}$ $\dot{q}$ $\dot{r}$. To estimate this signal, which is the derivative of the angular velocity signal $\omega = [p \quad q \quad r]^T$ recovered from the gyrometer, a new version of the adaptive differentiators sliding mode is proposed (see Fig. 7).

We propose the sliding mode surface from the differentiator:

$$s = z_0 - \omega. \quad (9)$$

The adaptive differentiator sliding mode is given by

$$\begin{aligned} \dot{z}_0 &= v_0, \\ v_0 &= z_1 - K.s - \hat{\lambda}_0 |s|^{\frac{1}{2}} \mathrm{sign}(s), \\ \dot{z}_1 &= -\hat{\lambda}_1 \mathrm{sign}(s), \end{aligned} \quad (10)$$

where $K \succ 0$.

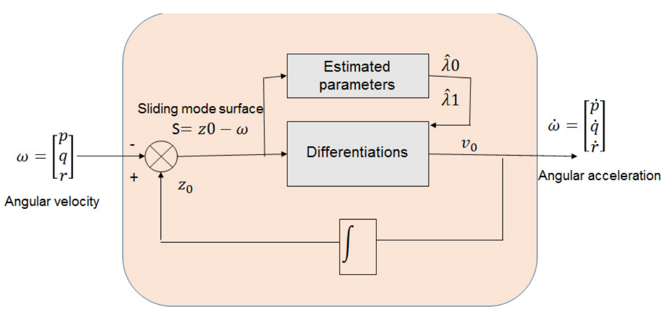

Fig. 7. Application of the adaptive differentiators for estimated angular accelerations $\dot{p}$, $\dot{q}$ et $\dot{r}$.

$z_0 = \begin{bmatrix} z_{0p} & z_{0q} & z_{0r} \end{bmatrix}^T$ is the estimated input angular velocity signal $\omega = [p \quad q \quad r]^T$.

$z_1 = \begin{bmatrix} z_{1p} & z_{1q} & z_{1r} \end{bmatrix}^T$ becomes equal to $v_0 = \begin{bmatrix} v_{0p} & v_{0q} & v_{0r} \end{bmatrix}^T$ and then constitutes the estimate of the derived angular acceleration signal $\dot{\omega} = \begin{bmatrix} \dot{p} & \dot{q} & \dot{r} \end{bmatrix}^T$. So, we have $z_1 = v_0 = \dot{\omega}$.

The dynamic adaptations of the gains $\hat{\lambda}_0$ and $\hat{\lambda}_1$ are given by

$$\begin{aligned} \hat{\lambda}_0 &= |s|^{\frac{1}{2}}.\mathrm{sign}(s).s, \\ \hat{\lambda}_1 &= s.\int_0^t \mathrm{sign}(s)dt. \end{aligned} \quad (11)$$

For the adaptive differentiator sliding mode algorithm, higher gains values λ_1 and λ_2 may be used to improve accuracy; however, this leads to an amplification of noise in the estimated signals. A good equilibrium between these two criteria (accuracy, robustness to noise ratio) is difficult to achieve. On the one hand, these values must increase the gains in order to derive a signal sweeping of some frequency ranges. On the other hand, low gains values have to be imposed to reduce noise amplification. So, our goal is to develop a differentiation algorithm in order to get a good compromise between error and robustness to noise ratio. To fit this requirement, a new version of differentiator with a sliding mode and a dynamic adaptation of the gains is proposed.

7.3.2. *Simulation's result*

The robust differentiator via sliding mode technique is used to recover the desired signal. Several flight tests were established to demonstrate the effectiveness of the combined adaptative/differentiator.

The desired signal injected p and the output differentiators are shown in Fig. 8.

We notice that the outputs of the differentiator z_{0p} follow the reference p perfectly.

The output differentiator z_{1p} and signal v_{0p} are shown in Fig. 9.

The signal z_{1p} follows v_{0p}. We notice that the sliding mode surface s_p is small (see Fig. 10).

The evolution of the $\hat{\lambda}_0$ is shown in Fig. 11.

7.4. ***Application of the TLSE technique for the aircraft aerodynamic model***

The TLSE technique is based on Singular Value Decomposition (SVD). This presents the advantage of obtaining the best approximation of the augmented measurements' matrix $[A \quad Y]$

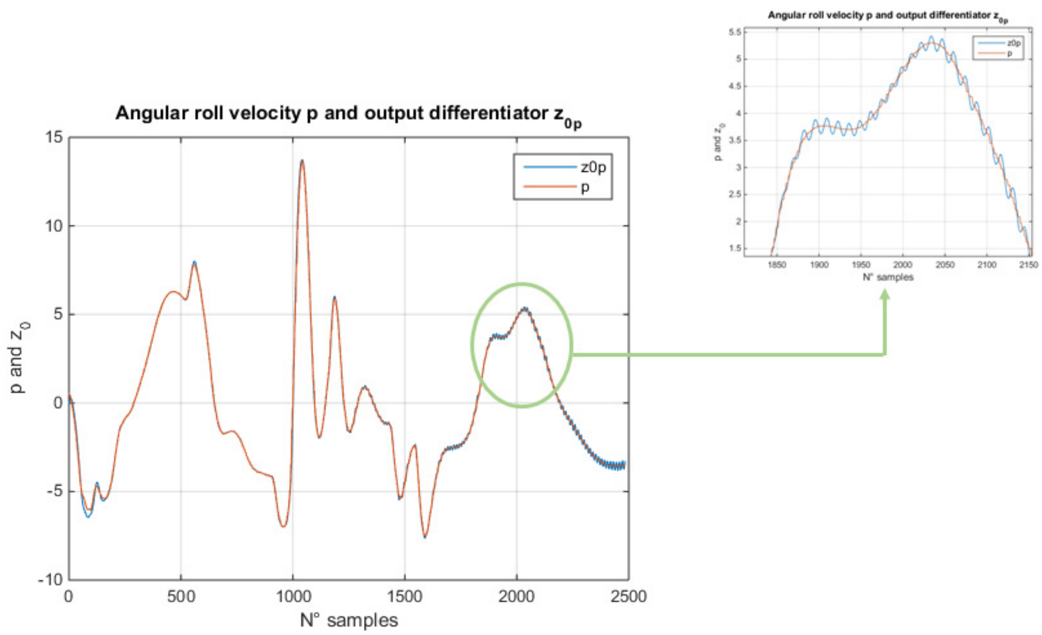

Fig. 8. Angular velocity p and output differentiator z_{0p}.

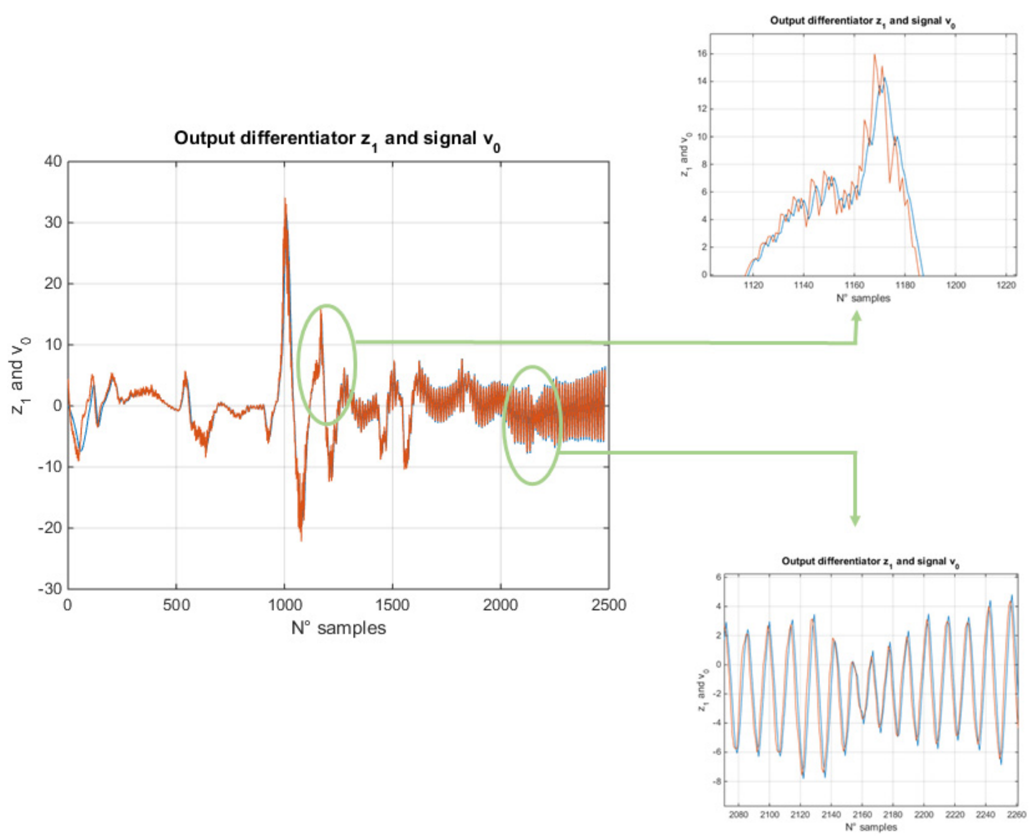

Fig. 9. Output differentiator z_{1p} and signal v_{0p}.

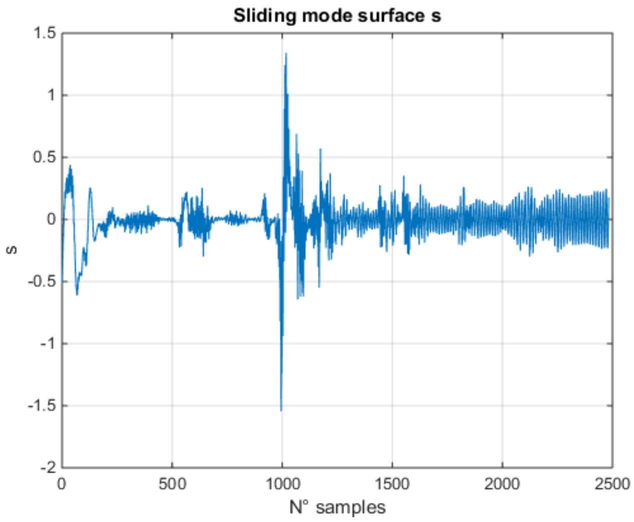

Fig. 10. Sliding mode surface s_p.

by another matrix with the same dimension but with a lesser large, where Y is the measurement vector defined as follows:

$$Y = \begin{bmatrix} C_D & C_L & C_m & C_l & C_y & C_n \end{bmatrix}^T. \tag{12}$$

and A is the (6×30) matrix defined as follows:

$$A = [A_1 \quad A_2]_{6\times 30},$$

$$A_1 = \begin{bmatrix} 1 & \alpha & i_H & \frac{qc}{V} & \delta_e & 0 & 0 & 0 & 0 & 0 & 0 & 0 & 0 & 0 & 0 \\ 0 & 0 & 0 & 0 & 0 & 1 & \alpha & i_H & \frac{qc}{V} & \delta_e & 0 & 0 & 0 & 0 & 0 \\ 0 & 0 & 0 & 0 & 0 & 0 & 0 & 0 & 0 & 0 & 1 & \alpha & i_H & \frac{qc}{V} & \delta_e \\ 0 & \dots & & & \dots & \dots & & & & & & & \dots & \dots & 0 \\ 0 & \dots & & & \dots & \dots & & & & & & & \dots & \dots & 0 \\ 0 & \dots & & & \dots & \dots & & & & & & & \dots & \dots & 0 \end{bmatrix}_{6\times 15},$$

$$A_2 = \begin{bmatrix} 0 & \dots & & & \dots & & & & & & & & \dots & \dots & 0 \\ 0 & \dots & & & \dots & & & & & & & & \dots & \dots & 0 \\ 0 & \dots & & & \dots & & & & & & & & \dots & \dots & 0 \\ \beta & \frac{pb}{2V} & \frac{rb}{2V} & \delta_a & \delta_e & 0 & 0 & 0 & 0 & 0 & 0 & 0 & 0 & 0 & 0 \\ 0 & 0 & 0 & 0 & 0 & \beta & \frac{pb}{2V} & \frac{rb}{2V} & \delta_a & \delta_e & 0 & 0 & 0 & 0 & 0 \\ 0 & 0 & 0 & 0 & 0 & 0 & 0 & 0 & 0 & 0 & \beta & \frac{pb}{2V} & \frac{rb}{2V} & \delta_a & \delta_e \end{bmatrix}_{6\times 15}. \tag{13}$$

Another advantage of the SVD is its ability to calculate an estimate of the invert of any matrix, whether it is singular or not.

The application of the TLSE technique for the estimation of aerodynamic coefficient's derivatives is presented. We summarize the method as follows:

Equations (2) and (4) can be represented using vector and matrix notation:

$$Y = A.\Theta, \tag{14}$$

where Θ is the (21×1)-dimensional vector of system parameters.

$$\Theta = \begin{bmatrix} C_{D_0} & C_{D_\alpha} & \dots & \dots & C_{n\delta_a} & C_{n\delta_r} \end{bmatrix}.^T \tag{15}$$

Rewrite the linear model of Eq. (11) as

$$[A \quad Y]\begin{bmatrix} \Theta \\ -1 \end{bmatrix} = 0. \tag{16}$$

The relation between true values and measured data is defined by the following equation:

$$[A_m \quad Y_m] = [A_0 \quad Y_0] + [\triangle A_0 \quad \triangle Y_0], \tag{17}$$

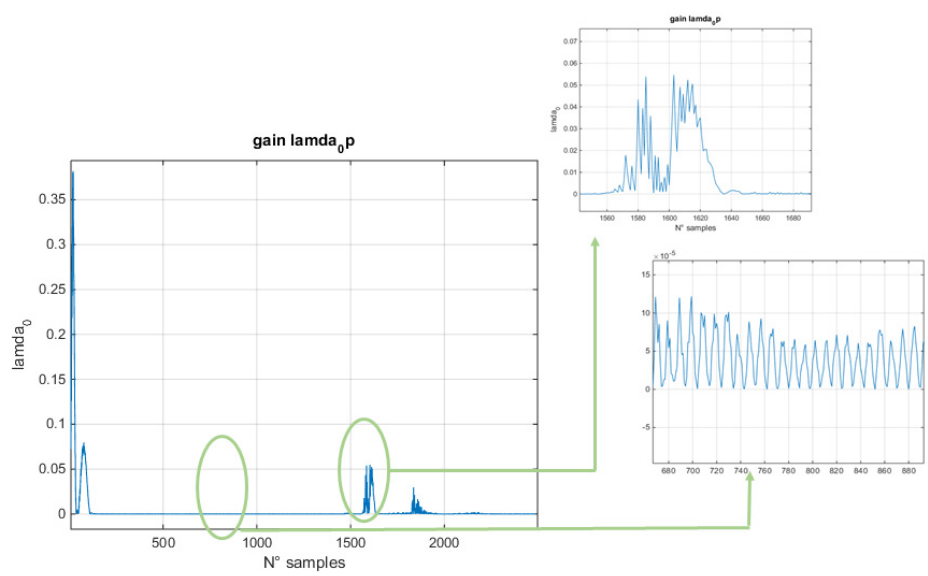

Fig. 11. Gain $\hat{\lambda}_0$.

where index m indicates the measurements, index 0 indicates the true values, and $\triangle$ indicates measurement errors.

Equation (11) is valid for the true data but not valid for the measured data:

$$\begin{aligned}\begin{bmatrix} A_0 & Y_0 \end{bmatrix}\begin{bmatrix} \Theta_0 \\ -1 \end{bmatrix} &= 0,\\ \begin{bmatrix} A_m & Y_m \end{bmatrix}\begin{bmatrix} \Theta \\ -1 \end{bmatrix} &\neq 0.\end{aligned} \tag{18}$$

The SVD of data matrix $\begin{bmatrix} A_m & Y_m \end{bmatrix}$ is defined by

$$\begin{bmatrix} A_m & Y_m \end{bmatrix} = U \begin{bmatrix} \sigma_1 & 0 & \dots & & & & \dots & 0 \\ 0 & \sigma_2 & \ddots & & & & & \vdots \\ \vdots & \ddots & \sigma_3 & & & & & \\ & & & \ddots & & & & \\ & & & & \ddots & & & \\ & & & & & \ddots & & \\ & & & & & \ddots & \ddots & \vdots \\ \vdots & & & & & \ddots & \ddots & 0 \\ 0 & & & & & \dots & 0 & \sigma_{n+1} \\ \dots & & \dots & \dots & \dots & \dots & & \dots \\ & & & & 0 & & & \end{bmatrix} V^T, \tag{19}$$

where $\sigma_1 \succcurlyeq \sigma_2 \succcurlyeq \dots \succcurlyeq \sigma_{n+1} \succcurlyeq 0$.

The last σ_{n+1} indicates the Frobenius norm distance of matrix $\begin{bmatrix} A_m & Y_m \end{bmatrix}$to the nearest rank deficient matrix.

The estimation of the minimum norm data correction matrix and the corrected data matrix is presented in the following equation:

$$\begin{aligned}&\begin{bmatrix} \triangle \hat{\mathrm{A}} & \triangle \hat{\mathrm{Y}} \end{bmatrix} \\ &= U \begin{bmatrix} 0 & 0 & \dots & & & & \dots & 0 \\ 0 & 0 & \ddots & & & & & \vdots \\ \vdots & \ddots & 0 & & & & & \\ & & & \ddots & & & & \\ & & & & \ddots & & & \\ & & & & & \ddots & & \\ & & & & & \ddots & \ddots & \vdots \\ \vdots & & & & & \ddots & 0 & 0 \\ 0 & & & & & \dots & 0 & \sigma_{n+1} \\ \dots & & \dots & \dots & \dots & \dots & & \dots \\ & & & & 0 & & & \end{bmatrix} V^T,\end{aligned} \tag{20}$$

$$\begin{bmatrix} \hat{\mathrm{A}} & \hat{\mathrm{Y}} \end{bmatrix} = U \begin{bmatrix} \sigma_1 & 0 & \dots & & & & \dots & 0 \\ 0 & \sigma_2 & \ddots & & & & & \vdots \\ \vdots & \ddots & \sigma_3 & & & & & \\ & & & \ddots & & & & \\ & & & & \ddots & & & \\ & & & & & \ddots & & \\ & & & & & \ddots & \ddots & \vdots \\ \vdots & & & & & \ddots & \sigma_n & 0 \\ 0 & & & & & \dots & 0 & 0 \\ \dots & & \dots & \dots & \dots & \dots & & \dots \\ & & & & 0 & & & \end{bmatrix} V^T. \tag{21}$$

The estimated parameters $\begin{bmatrix} \hat{\Theta}^T & -1 \end{bmatrix}$ of the system must satisfy the following equation:

$$\begin{bmatrix} \hat{\mathrm{A}} & \hat{\mathrm{Y}} \end{bmatrix}^T \begin{bmatrix} \hat{\Theta} \\ -1 \end{bmatrix} = 0. \tag{22}$$

Or

$$\begin{bmatrix} \hat{\Theta} \\ -1 \end{bmatrix} = \lambda.\mathrm{ker}\left\{\begin{bmatrix} \hat{\mathrm{A}} & \hat{\mathrm{Y}} \end{bmatrix}\right\}, \tag{23}$$

where λ is a scalar multiplier used to make the last element of v_{n+1} equal to -1.

The kernel of matrix $\begin{bmatrix} \hat{\mathrm{A}} & \hat{\mathrm{Y}} \end{bmatrix}$ equals the last right singular vector v_{n+1}.

7.5. *Simulation's results*

To determine the aerodynamic coefficients expressed in Eqs. (2), (4), (6) and (7), we have coded these equations as block diagrams in a RTWT module of Simulink/Matlab.

The Figs. 12 and 13 show the measured and estimated values of the longitudinal force coefficient C_x, the vertical force C_z, and the pitching moment coefficient C_m.

A positive correlation indicates that as the values of one variable increase, the values of the other variable increase, whereas a negative correlation indicates that as the values of one variable increase, the values of the other variable decrease.

Correlation coefficient is a measure of association between two variables, and it ranges between -1 and 1. If the two variables are in perfect linear relationship, the correlation coefficient will be either 1 or -1. The sign depends on whether the variables are positively or negatively related. The correlation coefficient is 0 if there is no linear relationship between the variables.

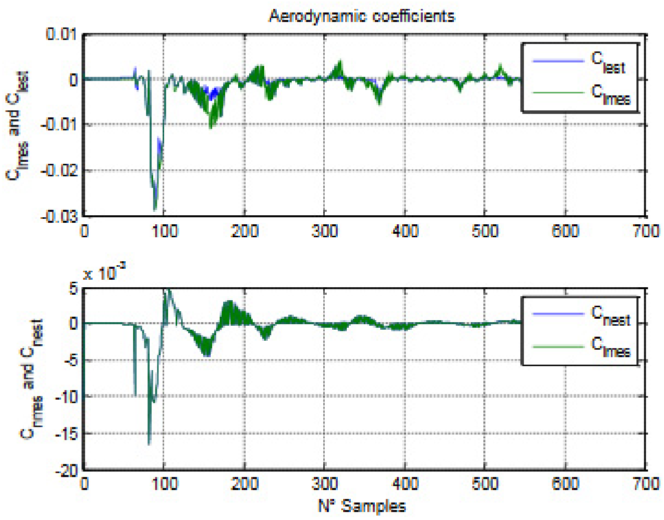

Fig. 12. Measured and estimated aerodynamic coefficients.

Finally, the goodness of fit the model can be expressed in terms of a correlation coefficient between Y and Y_{est}. This coefficient is usually referred to as the multiple correlation coefficient whose square is

$$R^2 = \frac{[Y_{\text{est}} - \bar{Y}]^T [Y_{\text{est}} - \bar{Y}]}{[Y - \bar{Y}]^T [Y - \bar{Y}]}, \tag{24}$$

where

$$\bar{Y} = \frac{1}{N} \sum_{i=1}^{N} Y_{\text{est}}(i). \tag{25}$$

In general, the estimated values of C_{xest}, C_{zest} and C_{mest} fit well with the measured values. The total correlation

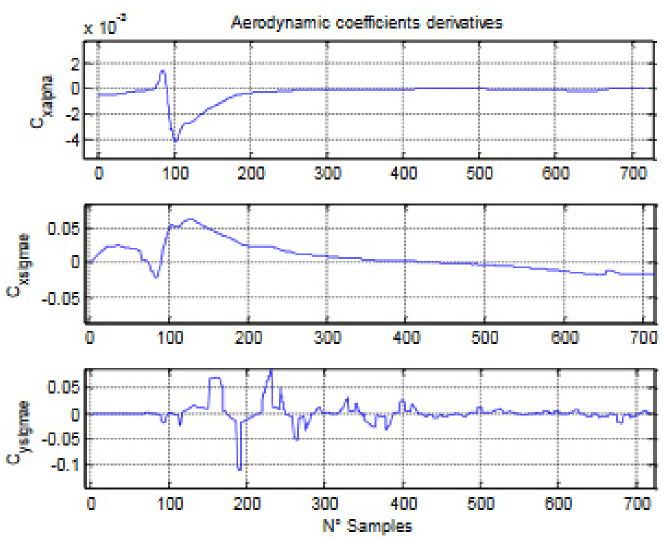

Fig. 13. Aerodynamic coefficients derivatives.

Table 2. Estimated aerodynamic coefficients.

Lift coefficients	Drag coefficient
C_{L_0} : 0.07	C_{D_0} : 0.071
C_{L_α} : 0.2	C_{D_α} : 0.007
C_{Li_H} : −0.9098	C_{Di_H} : 0.071
C_{Lq} : −3.909	C_{Dq} : 0.001
$C_{L\delta_e}$: −0.3727	$C_{D\delta_e}$: 0.009
Pitch coefficients	**Side force coefficients**
C_{m_0} : 0.07	C_{y_β} : −0.4
C_{m_α} : 5.21	C_{yp} : 0.043
C_{mi_H} : 0.491	C_{yr} : 0.049
C_{mq} : −9.658	$C_{y\delta_a}$: 0.18
$C_{m\delta_e}$: −0.758	$C_{y\delta_r}$: −0.02
Roll coefficients	**Yaw coefficients**
C_{l_β} : 0.073	C_{n_β} : 0.07
C_{lp} : −0.401	C_{np} : 0.06
C_{lr} : −0.021	C_{nr} : −0.2
$C_{l\delta_a}$: −0.301	$C_{n\delta_a}$: −0.3
$C_{l\delta_r}$: 0.026	$C_{n\delta_r}$: −0.028

coefficient R^2, see Eq. (24), of the force and moment coefficients is 0.8337, 0.9777 and 0.927, respectively.

We present some results of the obtained aerodynamic coefficients derivatives.

The mean values of aerodynamic coefficients are given in Table 2:

8. Aerodynamic Performance

The aerodynamic properties of aircraft wings are conducted by analyzing the lift and drag coefficients C_D, C_L.

8.1. *Lift versus AoA*

Theoretically, the lift curve shows a steady increase in the coefficient of lift C_L with an increase in the angle of attack α, up to the stall angle of attack. Beyond the stall angle of attack, the coefficient of lift decreases rapidly due to the stall of the airfoil.

Figure 14 is obtained by changing gradually the Angle of Attack (AoA) all over the flight, this procedure was possible by using the built-in autopilot available on the flight simulator. The flight tests then confirm that there is a proportionality between the lift coefficient and the angle of attack until the occurrence of the stall phenomenon. Beyond the stall angle of attack $\alpha_{\text{stall}} = 7.2^0$, the lift coefficient decreases rapidly.

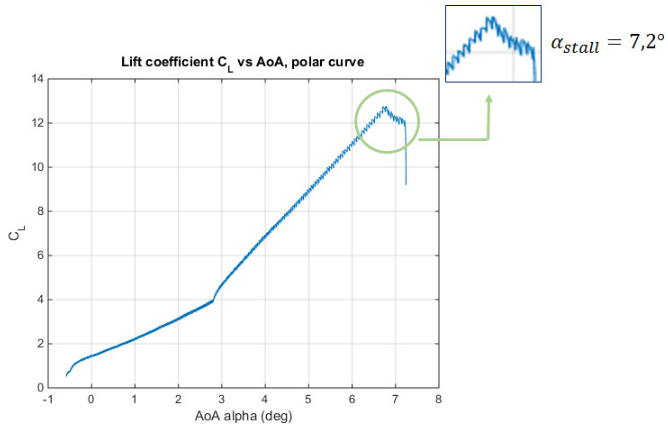

Fig. 14. Lift coefficient at different AoA, polar curve.

8.2. *Drag versus AoA*

The parabolic drag polar for the wing alone is written as

$$C_D = C_{D0} + \frac{C_L^2}{\pi.A.e}, \tag{26}$$

where A is the aspect ratio and $e = \frac{1}{1+\delta}$, $\delta \succ 0$. δ depends on the spanwise load distribution on the wing and e is called the oswald efficiency factor. It is generally obtained by plotting the total drag coefficient of the aircraft, obtained through measurements or estimates, against the square of the lift coefficient and fitting a straight line of linear variation range. Its value is generally less than unity and most researches on aircraft design recommend a value of the e in the range of 0.7–0.85 for preliminary design[11].

C_D versus C_L curve can be drawn. This means that for a given aircraft we can show how much drag is produced for a given lift at every angle of attack. This curve is called the polar curve.

For the different test flights used on the flight simulator, we obtained the polar curve shown in Fig. 15. Each point of the polar curve is obtained for a given angle of attack and shows the corresponding values of the coefficients of lift and drag.

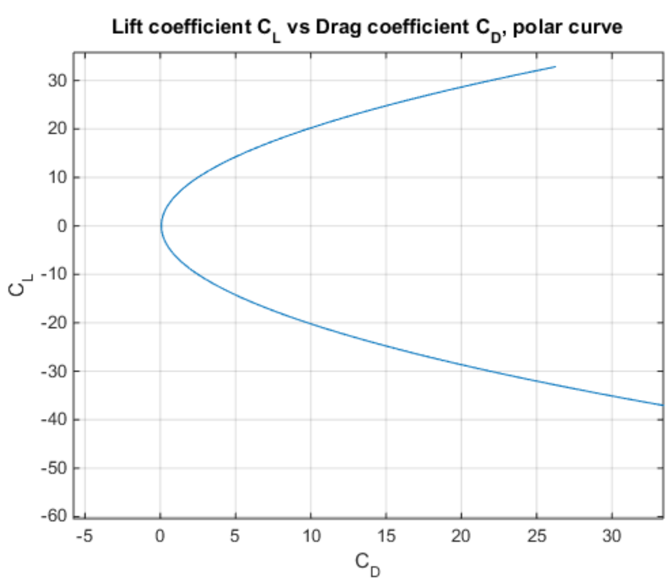

Fig. 15. Polar curve obtained by the flight test.

9. Conclusion

In this paper, a communication procedure with an aircraft virtual model in a simulated environment and the implementation of the real-time interface between the MSFS and the module RTWT of Simulink/Matlab have been presented. After that, the implementation of the aircraft aerodynamic model has been developed. Our solution uses the MSFS to minimize the complexity in design process.

As application on this simulator, two works have been presented, the first is reserved for the aerodynamic performances proposed to the academic world. The aircraft aerodynamic model is used to calculate the aerodynamic coefficients. The determination of the aerodynamic performances of the wing which are based on the polar drag, polar lift and the determination of the moment in which the aerodynamic stall phenomenon appears have been presented.

The second work, which is reserved for the estimation of the aerodynamic coefficients' derivatives, has been proposed to the research and development world, by means of the total least square technique. The piloting law expression is toughly tied to those derivatives which are unknown and usually unavailable.

The flight tests demonstrate the effectiveness of this new approach in identifying and evaluating the aircraft aerodynamic performances.

This work could be used as a new pedagogic approach, where the virtual simulation is employed to explore the aspect of aerodynamic coefficients.

References

[1] M. Laban, On-line aircraft aerodynamic model identification, Ph.D. Dissertation, (1994), doi:10.1016/S1474-6670(17)50633-3.
[2] J. Roskam, *Airplane Flight Dynamics and Automatic Flight Controls, Part I* (DARcorporation, 2001).
[3] H. Muhammad, H. P. Thien and T. Mulyanto, Total least squares estimation of aerodynamic parameter of micro coaxial helicopter from flight data, *Int. J. Basic Appl. Sci.* **12**(2) (2012).
[4] A. Jacek Goszczynski, Practical aspects of identification of the aerodynamic characteristics, *J. Theor. Appl. Mech.* **44**(1) (2006) 31–50.
[5] R. Louali, A. Belloula, M. S. Djouadi and S. Bouaziz, Real-time characterization of Microsoft Flight Simulator 2004 for integration into hardware in the loop architecture, in *Mediterranean Conf. Control and Automation (MED)* (IEEE, 2011), pp. 1241–1246, doi: 10.1109/MED.2011.5983151.

[6] M. Zaouche, A. Beloula, R. Louali, S. Bouaziz and M. Hamerlain, adaptive differentiators via second order sliding mode for a fixed wing aircraft, *CMES: Comput. Model. Eng. Sci.* **104**(3) (2015) 159–184, doi: 10.3970/cmes.2015.104.159.

[7] A. Hamissi, K. Busawon, L. Dala, Y. Bouzid, M. Zaouche and M. Hamerlain, A new nonlinear control design strategy for fixed wing aircrafts piloting, *Unmanned Syst.* **9**(4) (2020) 293–308, doi: 10.1142/S2301385021500126.

[8] D. J. Diston, Computational Modelling and Simulation of Aircraft and the Environment, *Platform Kinematics and Synthetic Environment*, Vol. 1 (Wiley, 2009), doi: 10.2514/4.867040.

[9] J.-L. Boiffier, *The Dynamics of Flight: The Equations* (John Wiley and Sons, 1998), pp. 92–94, doi: 10.1017/S0001924000064563.

[10] D. Allerton, *Principles of Flight Simulation*, (John Wiley and Sons, 2009), doi: 10.1002/9780470685662.

[11] I. Moir and A. Seabridge, *Aircraft Systems: Mechanical, Electrical, and Avionics Subsystems Integration*, 3rd edn. (Wiley, 2008), doi: 10.2514/4.479526.

[12] J. Guillaume and J. Ducard, *Fault Tolerant Flight Control and Guidance Systems: Practicals Methods for Small Unmanned Aerial Vehicles* (Springer, 2009), doi: 10.1007/978-1-84882-561-1.

[13] M. V. Bates and C. Hagstrom, *Flight Dynamics: Principles*, 2nd edn. (Elsevier, 2007), doi: 10.1016/C2010-0-65889-5.

[14] D. Bates and M. Hagstrom, *Nonlinear Analysis and Synthesis Techniques for Aircraft Control* (Springer, 2007), doi: 10.1007/978-3-540-73719-3.

[15] J. L. Junkins and H. Schaub, *Analytical Mechanics of Space Systems* (American Institute of Aerodynamics and Astronautics, 2002), doi: 10.2514/4.867231.

[16] J. Russell, *Performance and Stability of Aircraft* (Butterworth, Heinemann, 2003).

[17] T. Mung, *Aerial Vehicles* (In Tech, 2009).

[18] E. Torrenbeek and H. Wittenberg, *Flight Physics: Essentials of Aeronautical Disciplines and Technology with Historical Notes* (In Tech, 2009).

[19] D. P. Raymer, *Aircraft Design: A Conceptual Approach*, (American Institute of Aerodynamics and Astronautics, 1989), doi: 10.2514/4.869211.

[20] R. C. Nelson, *Flight Stability and Automatic Control* (McGraw-Hill Book Company, 1989), doi: 10.1017/S0001924000065362.

[21] S. M. Galhoun, *Six Degree of Freedom Modelling of an Uninhabited Aeriel Vehicle* (Cambridge University Press, 2007).

[22] M. Verhaegen, Filtering and system identification, Master thesis, Russ College of Engineering and Technology (2006). doi:10.1017/CBO9780511618888.

[23] A. Tewari, *Advanced Control of Aircraft, Spacecraft and Rockets* (John Wiley and Sons, 2011), doi: 10.1002/9781119971191.

[24] A. Tewari, *Automatic Control of Atmospheric and Space Flight Vehicles, Design and Analysis with MATLAB and Simulink* (Birkauser, 2011), doi: 10.1007/978-0-8176-4864-0.

[25] J. Roskam, *Airplane Aerodynamics and Performance, Part I* (DARcorporation, 1997).

[26] M. S. Grewal and A. P. Andrews, *Kalman Filetring: Theory and Practice using Matlab*, 2nd edn. (Wiley International Publication, 2001).

[27] R. Jategaonkar, *Flight Vehicle System Identification: a Time Domain Methodology* (American Institute of Aerodynamics and Astronautics, 2006), doi: 10.2514/4.102790.

[28] V. Klein and E. Morelli, *Aircraft System Identification: Theory and Practice* (American Institute of Aerodynamics and Astronautics, 2006), doi: 10.2514/4.861505.

[29] I. Markovsky and S. V. Huffel, Overview of total least-squares methods, *Signal Process.* **87**(10) (2007) 2283–2302, doi: 10.1016/j.sigpro.2007.04.004.

[30] S. V. Huffel and J. Vandewell, Analysis and properties of the generalized total least AX=B when some or all columns squares problem, in A are subject to error, *SIAM J. Matrix Anal.* **10**(3) (1989) 294–315.

[31] A. Gelb, *Applied Optimal Estimation* (Massachusetts Institute of Technology, Cambridge, Massachusetts; and London, England, 2001), Chap. 2,. doi: https://doi.org/10.1137/1019031.

[32] M. Zaouche, K. Foughali, M. Amini, Adaptive integral high-order sliding mode for a fixed wing aircraft, in *Recent Developments Sliding Mode Control: Theory and Applications*, Chap. 5 (Intech, 2017), pp. 87–104, doi: 10.5772/65568.